Title: More than germ cells: vascular development in the early zebrafish (*Danio rerio*) gonad

Authors: Michelle E. Kossack[1†], Lucy Tian[1], Kealyn Bowie[2], Jessica S. Plavicki[1*‡]

[1] Pathology and Laboratory Medicine Department, Brown University, Providence, RI

[2] Department of Ecology, Evolution, and Organismal Biology, Brown University, Providence, RI

* Corresponding Author: jessica_plavicki@brown.edu, 70 Ship St, Box G-E5, Providence, RI, 02903

[†] Supported by F32ES023650 and 5T32ES007272 both from NIEHS

[‡] Supported by NIEHS K99/R00 (ES023848), a CPVB Phase II COBRE (2PG20GM103652), and an NIEHS ONES award (ES030109)

Running Title: Vascular development in the early zebrafish gonad

Keywords: Zebrafish, bipotential gonad, endothelial, lymphatic, pericyte, macrophage, reproduction, single-cell, vasculature

Summary Sentence:

Delineating the complex cellular interactions between vascular and lymphatic endothelial cells, pericytes, and macrophage in the bipotential gonad is essential for understanding the differentiation and functioning of the mature gonad.

Abstract: Zebrafish are routinely used to model reproductive development, function, and disease, yet we still lack an understanding of the fundamental steps that occur during early bipotential gonad development, including when stromal cells invade the bipotential gonad to support gonad growth and differentiation. Here, we use a combination of transgenic reporters

and single-cell sequencing analyses to define the arrival of different stromal cell types to the larval zebrafish gonad. We determined that blood arrives to the gonad via the gonadal artery, which is derived from the swim bladder artery. We find that vascular and lymphatic development occurs concurrently in the bipotential gonad and our data suggest that, similar to what has been observed in developing zebrafish embryo, lymphatic endothelial cells can be derived from vascular endothelial cells. Although we established that *pdgfrb* expression is not exclusive to ovarian pericytes, we can resolve that *pdgfrb*+ pericytes support the migration of endothelial tip cells within the ovary. We observed that macrophage are the first stromal cell type to populate the zebrafish gonad, establishing a nascent resident population as early as 12 dpf. Further, macrophage are responsible for removing cellular material, particularly during sex differentiation. This foundational information demonstrates that the early bipotential gonad contains complex cellular interactions which may shape the health and function of the later gonad.

Introduction:

The developmental basis of the adult disease hypothesis postulates that the origins of some disease can be traced back to developmental changes, sometimes very subtle, that produce long-term cascading effects to ultimately alter organ function and health (1). Given their genetic similarity to humans, zebrafish have been extensively used to model early embryonic development (2). More recently zebrafish have also been used to model juvenile development and adult health, including gonadal formation and fertility (3–5).

The zebrafish gonad undergoes the same developmental stages as mammals; however, the timeline is elongated. The protracted developmental timeline allows for a detailed examination of very early periods of gonadal development, which have been understudied and may be sensitive to genetic and environmental disruptions. In mammals, primordial germ cells form at 7 days post conception (dpc) and, between ~9.5 and ~11.5 dpc, migrate from the

53 hindgut to the urogenital ridge (6–8). In mice, the primary sex-determining gene, *sex*
54 *determining region Y* (*Sry*), must be activated before 11 dpc to initiate the transition from a
55 bipotential gonad to a testicular development program (9). Since the mammalian bipotential
56 period only lasts <2 days, it can be difficult to investigate early sources of reproductive disease
57 that could occur during this critical developmental stage.

58 In the zebrafish, germ cells are specified at 4 hours post-fertilization (10). However, the
59 primordial germ cells (PGCs) remains quiescent while migrating into a position ventral to the
60 hind gut, a process which occurs from 1 day post-fertilization (dpf) to approximately 10 dpf (see
61 (11) for a detailed review). From 10 dpf until approximately 20 dpf, most of the germ cells
62 undergo mitosis, initiate meiosis, and remain in a bipotential state. Males and females maintain
63 a population of germline stem cells, which allow both sexes to produce new gametes throughout
64 their life. Zebrafish do not have a primary sex chromosome. Instead, during the biopotential
65 period, early-stage oocytes produce paracrine signals, which further support the development of
66 primary and secondary female sex characteristics (12,13). Around 20 dpf, in the presence of
67 sufficient oocyte-derived signaling, the oocytes continue to mature, growing larger, and,
68 ultimately, forming an ovary. In the absence of sufficient oocyte-derived signaling, oocytes
69 undergo apoptosis and the gonad will progress with a testicular developmental program (14,15).
70 Somatic cells receive germ cell-derived signals and respond by producing sex-specific factors
71 that further shape sexual differentiation (16). Somatic cells are shown in close association with
72 primordial germ cells as early as 4 dpf (17). By 11 dpf, these somatic cells have formed a
73 bilayer and begin to express sex specific markers (16). However, outside of these studies
74 nothing is known about the presents of other cell types at the biopotential gonad.

75 In mammals, a major area of research has been to delineate the role of support and
76 steroidogenic cells in sex determination and gonad maturation. Comparatively less has been
77 done to investigate the role of stromal cells (i.e., non-germ, non-support, and non-steroidogenic
78 cells) in the developing bipotential and differentiated mammalian gonad. Some research

79 indicates that additional cell types are present at early stages of gonad development. De Falco
80 et al. (18) found that macrophage are present at the urogenital ridge at E10.5, just prior to sex
81 determination, and that macrophage depletion limits vascular development. Brennan et al. (19)
82 found that, in contrast to previous ideas about the timeline of vascular development in the
83 mouse gonad, endothelial cells in XX and XY individuals are present by 11.5 dpc and form
84 lumenized vessels that are perfused with blood. The authors went on to show that vessel
85 formation is essential for testis development; however, considerably less is known about the
86 dynamics of vascular and other stromal cell development in the ovary. Recently, Garcia-Alonso
87 et al., (20) performed single-cell sequencing of the mouse gonad at 10.5 dpc and found many
88 different stromal cell types are present including vascular and lymphatic endothelium,
89 macrophage, and pericytes. Together, the presence of many different cell types suggests that
90 bipotential gonad health and later ovary and testis function may rely on complex interactions
91 between germ cells and stromal cells during the bipotential phase.
92 While it is known that the mature zebrafish ovary and testis contain endothelial and
93 lymphatic vasculature as well as perivascular cells and macrophage (21), the developmental
94 timeline for the arrival of these cell types to the developing gonad has not previously been
95 described. The long bipotential period of gonadal development in zebrafish compared to mice
96 provides an excellent opportunity to thoroughly assess the arrival of stromal cells prior to sex
97 determination. Using transgenic zebrafish with fluorescently expressed cellular markers, we
98 tracked the arrival of stromal cells to the bipotential zebrafish gonad. We found that the
99 bipotential gonad is more complex than originally considered, which suggests that additional cell
100 types have the potential to contribute to gonad development, sex determination, and fertility.
101
102 **Material and Methods:**
103 *Zebrafish Rearing*: Zebrafish (*Danio rerio*) were raised as described in Kossack et al. and
104 Westerfield (22,23). Larvae were placed in tanks at 5 dpf in 100mL rotifer culture, 400mL of fish

water static, and one drop of RG Complete (Reef Nutrition). From 5 to10 dpf, larvae were fed GEMMA Micro 75 (Skretting Zebrafish©) twice a day and live rotifers once a day. At 10 dpf, water flow was started as a slow drip, approximately one drop a second. From 10-20 dpf, fish were fed GEMMA Micro 75 twice a day, along with rotifers and artemia once a day. From 21 to 28 dpf, the water flow rate was increased until a standard flow rate was established. The fish were treated as adults at 90 dpf and fed GEMMA Micro 300 once a day.

Juvenile fish were euthanized according to procedures approved by the Institutional Animal Care and Use Committee at Brown University and adhered to the National Institutes of Health "Guide for the Care and Use of Laboratory Animals". In short, fish were placed in 0.04% MS-222 solution for 10-15 mins followed by ice water for 20 mins at which point they were decapitated and placed in 4% PFA overnight.

In establishing the developmental timeline, we measured the standard length of fish. The standard length is correlated with developmental stage during these ages (24,25). The full list of replicates, individuals, average length, and observations can be found in **Supplemental Table S1.**

Transgenic lines utilized: To mark vascular endothelial cells (VECs) we used three transgenic lines, *Tg(fli1:nEGFP)*^{y7}*, Tg(kdrl:GFP)* originally *Tg(flk1:GFP)*^{la116}*,* and *Tg(kdrl:DsRed2)* (26–28). Lymphatic endothelial cells (LECs) were labeled with *Tg(mrc1a:EGFP)* and *Tg(-5.2lyve1b:DsRed) (29,30)*. *Tg(piwil1:EGFP)* originally Tg(ziwi:EGFP) marked germ cells, and *TgBAC(pdgfrb:EGFP)* marked perivascular cells (31,32). In the study of macrophage we utilized *Tg(mpeg1:EGFP), Tg(mpeg1:Gal4FF)gl25,* and *Tg(UAS:Kaede)* (33,34). For readability and simplicity, we will refer to these transgenic lines by the simplified notations inside the parentheses, i.e *Tg(-5.2lyve1b:DsRed*) is listed as *lyve1b:DsRed*.

130 *Antibody Staining*: Antibody staining for germ cell protein Vasa was performed as described in
131 Leerberg et al. (16) using anti-Vasa antibody from GeneTex (GTX1238306) at a working
132 concentration of 1:1000. All secondary antibodies were used at 1:500 and are as follows: goat
133 anti-rabbit IgG 488 (Thermo Fisher Scientific Cat# A-11034, RRID:AB_2576217) and goat anti-
134 rabbit IgG 633 (Thermo Fisher Scientific Cat# A-21071, RRID:AB_2535732). After protein
135 labeling, tissues were stained with Hoechst 33342 (Invitrogen H3570) at a concentration of
136 1:10,000 overnight, dissected, and placed in Vectashield mounting media (Fisher Scientific,
137 NC9265087) for subsequent imaging.
138
139 *Photoconversion and live imaging*: Double transgenic line *mpeg1:GAL4;UAS:Kaede* fish were
140 identified at 3 dpf. At 12 dpf, fish were anesthetized in 0.02% MS222 for 1 minute then mounted
141 on a 35mm glass bottom microwell dish (MatTek, Part No. P35G-1.5-14-C) in 2% low-melting
142 temperature agarose (Fisher Scientific, bp1360-100) made in egg water (4 parts per thousand
143 salt). The mounted fish was surrounded in 0.02% MS-222 and placed on the confocal
144 microscope. Using 20x objective, the mid-section of the fish was exposed to full-power LED
145 405nm fluorescent light for 60 seconds to photoconvert the Kaede from green to red. The fish
146 was immediately removed from agarose and replaced in the tank. The tank was covered with
147 foil to protect the fish from additional light during transportation back to the fish facility. 24 hours
148 later, the fish were again anesthetized and mounted laterally in agarose. Using a 20x objective,
149 *piwil1:EGFP* expressing fish were identified from the previously photo-converted fish and
150 imaged.
151
152 *Imaging*: Images were collected on a Zeiss LSM 880 confocal microscope. Maximum intensity
153 projections, orthogonal slices, and colocalization analysis were performed with ZenBlack
154 (Zeiss). Tissues from 10 – 15 dpf zebrafish were mounted on Premium microscope slides
155 (Fisher Scientific, 12-544-7) with Premium cover glass (Fisher Scientific,12-548-B) held in place

156 by vacuum grease. Tissues >20 dpf were mounted in 1% low-melting agarose in a 35mm glass
157 bottom microwell dish.
158
159 *Sequencing Analysis*: From Liu et al., (21) we obtained matrixes of gene and feature count.
160 These large matrixes gathered from raw single-cell sequencing data display individual cells on
161 one axis vs. counts of every gene detected in the other. From this data we are able to perform
162 principal component analysis to group similar cells together, which is referred to as clustering.
163 For more details about the analysis see Seurat (35,36), and R code
164 (https://repository.library.brown.edu/studio/item/bdr:d4ef3vpa/). Clustering of the ovarian cells
165 was performed as described in Liu et al. and cluster 5 was identified as the "Blood Vessel"
166 cluster as described in the publication (21). We isolated this group using the subset() function
167 and looked at the expression of VEC and LEC markers. We attempted sub-clustering analysis,
168 but there were insufficient cell numbers within this cluster alone to draw meaningful information.
169 To generate the pericyte Venn diagram, we used publicly available data from Liu et al.
170 and Shih et al. (21,37). Briefly, both publications included lists of highly expressed genes
171 identified in all cell type. We, therefore, were able to download the list of genes expressed in the
172 cell types of interest, filter them for expression level, and compare the lists. From Liu et al. (21),
173 we downloaded the dataset of differentially expressed genes in stromal cells (from
174 Supplemental Table 5) and filtered the data to only include genes whose p_val_adj<0.05. We
175 called this group "ovarian stromal cells". We applied the same filtering parameters to narrow
176 down the "ovarian pericytes" (sub-cluster 2). We eliminated duplicates within each list to
177 generate 2,606 genes in the ovarian stromal cell group and 441 genes in the ovarian pericyte
178 group.
179 Similarly, using publicly available data from Shih et al. (37), we downloaded the highly
180 expressed genes identified in all pdgfrb-expressing cells (from Supplemental Table S2.1). As
181 described in the publication we filtered for expression level $\log_2>1$, this list of genes was defined

182 as "*pdgfrb*+ cells". We performed the same methodology to Table S1.4, which was identified as
183 "cluster 39". We eliminated duplicates within each list, which resulted in 2,084 genes in *pdgfrb*+
184 cells and 105 genes in cluster 39. Using the list comparison tool (https://rnact.crg.eu/compare),
185 we found the overlapping and unique genes for each group. These numbers were used to
186 create the Venn diagram using Venn.Plot in R studio. List details are available in **Supplemental**
187 **Table S2**.
188
189
190 **Results**:
191 *Vascular endothelial cells make initial contact with the anterior gonad*
192 To establish a timeline of vascular development in the gonad, we used a double
193 transgenic line *kdrl:DsRed; fli1:nEGFP* that carries both the pan-endothelial marker *fli1:nEGFP*
194 as well as *kdrl:DsRed*, which marks vascular endothelial cells (VECs). Beginning at 10 dpf, we
195 used a qualitative scale to measure the distance between the gonad, marked by germ cells, and
196 the VECs. We defined the relationship between the cells using three categories, "No Contact"
197 (**Figure 1A**), "Proximal" (near, but not physically associated, **Figure 1B**), or "Contact" (**Figure**
198 **1D, Supplemental Figure S1**). We found that in most individuals (n=15/17), VEC contact with
199 the germ cells occurred by approximately 20 dpf (**Figure 1F**), which corresponded to a standard
200 length of 7.21± 0.666mm (**Figure 1G, Supplemental Table S1**). We observed that the initial
201 VECs contact occurred with the anterior most portion of the developing gonad (**Figure 1E**). Prior
202 to this study, it was not known which vessels supplied blood to the bipotential gonad. We
203 determined that at 20 dpf the blood supply to the bipotential gonad originates from the swim
204 bladder artery (**Figure 1H**). Posterior to the anterior chamber of the swim bladder, the swim
205 bladder artery divides, with two different branches supplying blood to the right and left gonad
206 (**Figure 1H**). We termed this artery the gonadal artery.
207

208 *Specification of lymphatic endothelial cells in the gonad resembles embryonic lymphatic*
209 *development*

210 The role of the lymphatic vasculature in organogenesis and homeostasis has been
211 understudied in zebrafish (38). Recent single-cell sequencing of the zebrafish ovary found that
212 lymphatic endothelial cells (LECs) are present in the ovary by 40 dpf (21); however, it is not
213 known when lymphatic cells invade the ovary and create functional networks within it. To
214 determine when VECs and LECs reach the ovary, we visualized the endothelium by crossing
215 canonical vascular endothelial reporter lines *kdrl:GFP* or *kdrl:DsRed* with established lymphatic
216 endothelial transgenic reporters, *mrc1a:EGFP* or *lyve1b:DsRed* (29). Using this double
217 transgenic approach, we determine that LECs are detected in the gonad at 20 dpf, the same
218 time as VECs (**Figure 2A, 2B,** 20 dpf, standard length of 7.17±1.04mm, n=13/13,
219 **Supplemental Table S1**).

220 It is unclear from our analysis of early stromal colonization of the gonad if VECs give rise
221 to LECs or if the lymphatic endothelium enters the gonad independent of the vascular
222 endothelium. During embryonic development, LECs are derived from venous VECs (30,39–46).
223 *flt4*, a marker of venous endothelial cells and LECs, is required for initiating LEC development.
224 Expression of *flt4* is followed by the expression of *prox1a*, which specifies the lymphatic fate in
225 mammals (46–53). However, in other contexts, such as anal fin vascularization, VECs are
226 derived from LECs (52). To gain insight into which mechanism might be utilized in the gonad,
227 we mined previously available single-cell sequencing from the 40 dpf zebrafish ovary (21). We
228 sub-clustered the vasculature ("Blood Vessels") and looked for expression and co-localization of
229 specific endothelial markers. We found VEC markers *kdrl*, *fli1*, and *flt1*, to be expressed in the
230 majority of cells (**Figure 3A**) whereas *lyve1b*, *flt4*, and *prox1a* were expressed in a smaller
231 subset of cells (**Figure 3B**). Next, we assessed whether *kdrl* and *lyve1b* were co-expressed in
232 this cluster and we found no overlap in expression (**Figure 3C**). However, *lyve1b* was co-
233 expressed with the venous marker *flt4*, suggesting that lymphatic development in the gonad

234 may occur in a manner similar to what has been observed in the embryonic endothelium (29).
235 We note that we were not able to examine the expression of *mrc1a* in the single-cell sequencing
236 data set because it was not detected in the original sequencing analysis.
237 To assess if LECs were derived from VECs in the bipotential gonad, we used confocal
238 microscopy to image 20 dpf gonads expressing transgenic markers for both VECs and LECs
239 (*kdrl:DsRed; mrc1a:EGFP*). Our imaging revealed overlap in the *kdrl:DsRed* and *mrc1a:EGFP*
240 expression domains (**Figure 4A**). However, in most of the cells that expressed both genes, the
241 level of transgenic expression was not equal, and we consistently observed expression of one
242 marker being dominant over the other in the maximum intensity projection (**Figure 4B and 4C**).
243 Orthogonal slices of the z-stacked images illustrate that the incongruent levels of expression
244 between markers is not an artifact of the maximum intensity projection (**Figure 4D**). Finally, we
245 used Zen Black to perform a co-localization analysis of the confocal images and found that
246 although the *mrc1a:*EGFP expression obscured the visibility of the *kdrl:DsRed*, there was 100%
247 overlap in signal (**Figure 4E,** Overlap coefficient = 0.97). Together this supports that LECs in
248 the 20 dpf zebrafish gonad are derived from VECs, and as lymphatic specific expression
249 increases, vascular endothelial expression decreases.
250
251 *Pdgfrb+ perivascular cells associate with vascular tip cells invading the bipotential gonad*
252 Pericytes are a sub-type of mural cells that have since their discovery been difficult to
253 clearly distinguish from other perivascular cell types (54). In the developing zebrafish embryo,
254 pericytes were originally defined by expression of *pdgfrb*, their morphology, and their positional
255 relationship to the vasculature. However, recent evidence from embryonic zebrafish indicates
256 that while pericytes tend to have the highest *pdgfrb* expression they constitute only a subset of
257 the *pdgfrb*:EGFP+ cells (37). Similarly, single-cell sequencing of the ovary showed that *pdgfrb+*
258 cells are found in multiple clusters of stromal cells. In this larger group, pericytes were better
259 defined by the expression of *plp1b*, a sub-cluster with high *pdgfrb* and *notch3* expression (21).

260 To determine if there was a pericyte marker unique to the gonad and not expressed in embryos,
261 we compared expression of embryonic *pdgfrb*:EGFP cells and cluster 39 (highest *pdgfrb*
262 expression (37)) with ovarian stromal cells (*pdgfrb*+ cells (21)) and ovarian pericytes (*plp1b*+
263 (21)). We did not identify gene expression signatures that were unique to ovarian pericytes
264 (**Figure 5**); however, eight genes were found to be co-expressed in cluster 39, ovarian stromal
265 cells, and ovarian pericytes (a complete list of overlap in **Supplemental Table S2**). These eight
266 genes did not include the ovary pericyte-specific marker *plp1b*, this suggests either that ovarian
267 pericytes have unique functions not shared by embryonic pericytes, or that the function of *plp1b*
268 in the ovarian pericytes is not intrinsic to pericytes.
269 As with all vascular beds, pericytes in the ovary are an essential part of the vascular unit,
270 creating stability for the constant vascular modeling that occurs as an inherent part of ovarian
271 function (as reviewed in (55). Since *pdgfrb* is an imperfect marker of pericytes, we used the
272 double transgenic *pdgfrb:EGFP;kdrl:DsRed* to determine if *pdgfrb*+ cells within the gonad were
273 also in contact with a vessel. We found that oblong *pdgfrb*+ cells are associated with vessels in
274 the developing gonad and based on their gene expression, position, and morphology, appeared
275 to be pericytes. The *pdgfrb*+ presumptive pericytes arrived at the gonad along with the
276 endothelial cells (**Figure 2A,** 20 dpf, 7.61±0.515mm, n=8/9, **Supplemental Table S1**). Confocal
277 images revealed projections extending from *pdgfrb*+ cells between *kdrl*+ vessels (**Figure 6**),
278 suggesting that pericytes may aid in the migration of vascular tip cells, which has been
279 observed during the vascularization of other tissues (32,56).
280
281 *Macrophage arrive at the bipotential gonad prior to other stromal cells types*
282 Lastly, we investigated the arrival of macrophage to the gonad. Macrophage are known
283 to play a substantial role in both ovary and testis function in mammals, however their
284 colonization of the zebrafish gonad remains unclear (57–59). We found that while macrophage
285 colonization of the gonad in most individuals was concurrent with vascularization of gonad, in

286 some cases we observed macrophage within the gonad prior to vascularization (**Figure 2A,** 12
287 dpf, 4.74±0.849mm, n=6/14, **Supplemental Table S1**). Notably, we found that at 20 dpf, when
288 the gonad is undergoing sex determination, there are more macrophage present, and they can
289 be seen engulfing germ cells (**Figure 7B,C**). This suggests that macrophage may play an active
290 role in gonad differentiation in zebrafish.

291 Finally, we asked if the macrophage that make initial contact with the gonad became
292 resident macrophage or if they were only transiently interacting with the germ cells. Given the
293 superficial position of the macrophage in contact with the early gonad (**Figure 7A**), we
294 hypothesized that macrophage found during the bipotential stage were not tissue-resident and
295 the resident population would not be established until after sex determination. To test this
296 hypothesis, we used a pan-macrophage reporter to drive expression of Kaede *(mpeg1:GAL4;*
297 *UAS:Kaede)*, a photoconvertible fluorescent protein that changes from green to red following
298 exposure to 405nm light. We exposed fish at 12 dpf to 405nm light in a defined region
299 surrounding the gonad. As a result, macrophage in and near the gonad were converted to red,
300 leaving the remaining macrophage in the body green. 24 hours later we used live imaging to
301 observe the macrophage population within the gonad. The presence of only red macrophage
302 would indicate that no new macrophage had entered the gonad and suggest that macrophage
303 become resident prior to sexual differentiation. The presence of green macrophage in addition
304 to red macrophage would indicate either: (1) continued colonization of the gonad, (2) the
305 presence of transient populations of macrophage, or (3) newly divided macrophage from a
306 previously photoconverted cell although likely some red would remain from the mother cell. We
307 found that after 24 hours, a subset of macrophage were retained in the gonad and expressed
308 the red photoconverted kaede protein (**Figure 7E,** red arrowhead, n=5). We also observed
309 green macrophage in and in the proximity of the gonad (**Figure 7F,** green arrow). Finally,
310 several cells also were green and red mixed suggesting that they had some previous
311 conversion while generating new Kaede protein (**Figure 7D,** blue arrow). It is difficult to say

312 where the double-labeled cells originated. Given the ratio of green to red in these cells it is most
313 likely that these cells were on the periphery of the conversion area and migrated to the gonad
314 while producing new Kaede protein. Together, these data suggest that at 12 dpf, there is an
315 early population of resident macrophage that cells within the bipotential gonad.
316
317 **Discussion**:
318 Here we provide the first report of vascularization of the early zebrafish gonad, a
319 fundamental and understudied component of reproductive development and health. We found
320 that vascular endothelial cells and lymphatic endothelial cells are present in the ovary by 15 dpf.
321 In mammals, two previous studies tracked the arrival of endothelial cells to the early gonad
322 (19,60). Both studies found that by 11.5 dpc endothelial cells, marked by Tie-2, Flt1, and
323 PECAM, were present in the gonad. However, neither publication examined earlier time points
324 until Garcia-Alonso et al. (20) performed single-cell sequencing on 10.5 dpc mice. In this data
325 set, we can query markers for stromal cell types and find all are present, however, this
326 methodology lacks spatial resolution. Based on these previous studies, we can conclude that
327 vascularization during the bipotential phase of gonad development is very similar between
328 zebrafish and mammals. Although our investigation clearly indicates VECs and LECs are
329 present in the bipotential gonad, it does not evaluate when the vessels establish a functional
330 network. Future investigations will be required to determine when the vessels are lumenized
331 and are able to transport physiological signals and waste.
332 Prior mammalian studies used pan-endothelial cell markers and, therefore, these studies
333 do not allow us to distinguish between endothelial cell types during gonad development (61,62).
334 In adult mice, LECs and VECs have distinct domains in both the ovary and testis (19,62), but
335 the establishment of these domains early in development is unclear. In mice, Brennen et al. (19)
336 found that LECs, marked by Prox1$^{+/lacZ}$, are present in the mesonephros at 13.5 dpc and enter
337 the gonad at 17.5 dpc in both sexes. However, using a transgenic Prox1-EGFP mouse,

338 Svingen et al. found that the ovary does not contain LEC until after birth at post-natal day 10,
339 while the testis contains LEC by 17.5 dpc (62). Yet murine expression analysis using single-cell
340 sequencing shows evidence of *prox1* expression in the gonad at 10.5 dpc (20). Each of these
341 studies used different methods and criteria (lacZ, transgenic line, mRNA expression,
342 respectively) to determine the presence of LEC in the gonad using *Prox1*. Therefore, the
343 observed discrepancies could be due to differences in methodology or criteria. When comparing
344 zebrafish to mice, it becomes more difficult to assess the parallels between these two model
345 species. Most mammalian studies use *Prox1* as the LEC marker. In our study, we defined LECs
346 to be *mrc1a* or *lyve1b* expressing cells, because *prox1* is known to be expressed in a number of
347 different ovarian cell types and is not required for lymphatic cell specification in zebrafish
348 (44,49). Single-cell sequencing is able to detect extremely low expression of *Mrc1* and *Lyve1*
349 (the mammalian orthologs of mrc1a and lyve1b respectively) at 10.5 dpc, which suggests the
350 earlier timeline of LEC arrival seen in zebrafish also occurs in mammals (20).
351 We also demonstrated that the *pdgfrb* expression domain within the ovary is not limited
352 to pericytes and likely includes other mural cells with different sub-functionalizations. We show
353 that *pdgfrb*+ cells extend between vessels within gonad, which likely reflects pericytes extending
354 to support migrating vascular tip cells, a phenomenon that has been observed in other
355 developmental contexts (32,56). Vascular tip cells release *pdgf* ligands which signal
356 perivascular cells to follow and stabilize the forming vessel. When performing confocal analysis
357 of the tissue morphology, we kept detection levels controlled to accurately represent the
358 pericyte morphology. In this case if we overexposed the channel, we were able to see some
359 *kdrl:DsRed* adjacent to the *pdgfrb*+ cell (data not shown). Likely we are limited by the thickness
360 of the tissue, and strength of the DsRed fluorophore.
361 Pericyte biology is still relatively nascent and *pdgfrb* has been routinely used as the
362 primary marker across species. In embryonic zebrafish, *pdgfrb* is required for the formation of
363 the intersegmental vessels and meningeal angiogenesis (63,64). In other species, it is known

364 that pericytes are essential for vascular stability and reconstruction of the ovarian vasculature
365 during follicle development and post-ovulation (65–68). Consistent with this finding, inhibition of
366 PDGFR in the rat ovary causes hemorrhaging (69). Together, these reports indicate a role of
367 pericytes in the function and establishment of the blood follicle barrier (70,71). When we
368 compared the gene expression profiles of pdgrfb+ cells in cluster 39, ovarian stromal cells, and
369 ovarian pericytes, we found that eight genes were shared between cluster 39, ovarian stromal
370 cells, and ovarian pericytes. Of these, we noticed two were associated with cell adhesion
371 (*pcdh1b* and *s1pr1*). *s1pr1* has been shown to play critical roles in negatively regulating
372 angiogenesis in zebrafish (72) and knockout of S1pr1 in mice causes size-selective openings in
373 the blood-brain barrier (73). Although it is likely that *s1pr1* is not specific to pericytes, as it is
374 also expressed in VEC including hepatocellular carcinoma (74), the shared expression of cell
375 adhesion genes in cluster 39 and ovarian pericytes supports the idea that pericytes play a
376 critical role in the blood follicle barrier development in zebrafish. It will be necessary to
377 understand how pericytes interact with the ovarian vasculature, particularly in addressing
378 ovarian disease. Both ovarian hyperstimulation syndrome and polycystic ovary syndrome are
379 associated with altered ovarian vasculature (75–77). Although it is well established that
380 pericytes perform a critical role in vascularization and angiogenesis, the role that perivascular
381 cells play in disease etiology remains unclear (reviewed in (76)). Zebrafish are able to model
382 ovarian diseases such as PCOS (78), therefore the discovery of stromal cells in the bipotential
383 gonad offers an opportunity to investigate the role of these cells in the very early reproductive
384 disease formation.

385 We discovered that macrophage are present in the early bipotential gonad and can be
386 seen engulfing germ cells during the bipotential phase. In mice, yolk-sac-derived macrophage
387 are responsible for clearing cellular debris from endothelial cells, Sertoli cells and germ cells, as
388 well as for pruning vascular networks in the testis (18). In other contexts, macrophage are
389 known to release angiogenic cues that shape vascular development (79–83). Therefore, their

390 presence in the bipotential gonad prior to the arrival to VECs could suggest that macrophage
391 could be involved in directing vascularization of the gonad. While ovarian resident macrophage
392 are essential for folliculogenesis, ovulation, and the clearing of atretic follicles (59,84,85) and
393 cellular debris (58), prior to this study, macrophage phagocytosis in the zebrafish ovary had not
394 been observed. We also report that gonad resident macrophage are present by 12 dpf and the
395 population is dynamic during this developmental window with new macrophage migrating into
396 and out of the gonad. In mice, ovarian resident macrophages can be divided into 5 different
397 populations. Two of these initial subpopulations are embryonically derived, one population from
398 the yolk-sac and the other from the fetal liver (58). However, the majority of research studies
399 have investigated resident macrophage function after sex determination. The presence of
400 macrophage in the zebrafish bipotential gonad, suggests that macrophage may also be present
401 in the mammalian bipotential gonad and contribute to important steps in sexual differentiation.
402 In conclusion, we found that stromal cells begin populating the bipotential gonad at 12
403 dpf. Our data suggest that VEC give rise to LEC in the gonad and create a complex network of
404 endothelial cells by 20 dpf, however, it is still unclear when these vessels become functional
405 conduits for physiological signals and nutrients. We found that *pdgfrb* support the migration of
406 vascular tip cells; however, a more specific ovarian pericyte marker is needed to understand the
407 role of pericytes vs. *pdgfrb* expressing cells in ovarian development. Finally, we found that
408 tissue resident macrophage can be found in the gonad as early as 12 dpf and are important for
409 clearing oocyte debris during sexual differentiation. Our foundational information regarding
410 stromal cell invasion into the biopotential gonad contributes to the understanding of the early
411 bipotential environment and how it may contribute to the etiology of reproductive disease.
412

413 **Acknowledgments**:
414 We would like to thank Rachel Cyr for all her meticulous work caring and raising the fish. We
415 would also like to thank the Weinstein and Draper labs for sharing their transgenic lines that

made this study possible. Thank you to Dr. Bruce Draper and Dr. Daniel Spade for their comments on the manuscript. This work was made possible by funding from NIEHS to Dr. Michelle Kossack F32ES023650 and 5T32ES007272. Dr. Jessica Plavicki was supported by an NIEHS K99/R00 (ES023848), a CPVB Phase II COBRE (2PG20GM103652), and an NIEHS ONES award (ES030109).

Data Availability:

The data underlying this article are available in the Brown Digital Repository at: https://repository.library.brown.edu/studio/item/bdr:d4ef3vpa/

Conflict of Interest Statement:

MEK, LT, KB, and JSP have no conflicts of interest to declare.

Author Contribution:

MK: Conceptualization, methodology, investigation, writing – original draft, review, and editing, visualization. LT and KB: Investigation, writing – review and editing. JSP: Resources, writing – review and editing, supervision, project administration, fund acquisition.

References:

1. De Boo HA, Harding JE. The developmental origins of adult disease (Barker) hypothesis. Aust N Z J Obstet Gynaecol. 2006 Feb 1;46(1):4–14.

2. Howe K, Clark MD, Torroja CF, Torrance J, Berthelot C, Muffato M, et al. The zebrafish reference genome sequence and its relationship to the human genome. Nature. 2013;496(7446):498–503.

3. Baker TR, Peterson RE, Heideman W. Early Dioxin Exposure Causes Toxic Effects in Adult Zebrafish. Toxicol Sci. 2013 Sep;135(1):241–50.

4. King Heiden T, Carvan MJ, Hutz RJ. Inhibition of follicular development, vitellogenesis, and serum 17β-estradiol concentrations in zebrafish following chronic, sublethal dietary exposure to 2,3,7,8-tetrachlorodibenzo-p-dioxin. Toxicol Sci. 2006;90(2):490–9.

5. King Heiden TC, Spitsbergen J, Heideman W, Peterson RE. Persistent adverse effects on health and reproduction caused by exposure of zebrafish to 2,3,7,8-Tetrachlorodibenzo-p-dioxin during early development and gonad differentiation. Toxicol Sci. 2009;109(1):75–87.

6. Bendel–Stenzel M, Anderson R, Heasman J, Wylie C. The origin and migration of primordial germ cells in the mouse. Semin Cell Dev Biol. 1998 Aug;9(4):393–400.

7. McLaren A, Durcova-Hills G. Germ cells and pluripotent stem cells in the mouse. Reprod Fertil Dev. 2001;13(8):661.

8. Wilhelm D, Palmer S, Koopman P. Sex Determination and Gonadal Development in Mammals. Physiol Rev. 2007 Jan 1;87(1):1–28.

9. Hiramatsu R, Matoba S, Kanai-Azuma M, Tsunekawa N, Katoh-Fukui Y, Kurohmaru M, et al. A critical time window of Sry action in gonadal sex determination in mice. Development. 2009;136(1):129–38.

10. Yoon C, Kawakami K, Hopkins N. Zebrafish vasa homologue RNA is localized to the cleavage planes of 2- and 4-cell-stage embryos and is expressed in the primordial germ cells. Development. 1997;124(16):3157–65.

11. Michelle E. Kossack, Bruce W. Draper. Genetic regulation of sex determination and maintenance in zebrafish (Danio rerio). Curr Top Dev Biol. 2019;134:119–49.

12. Dranow DB, Hu K, Bird AM, Lawry ST, Adams MT, Sanchez A, et al. Bmp15 Is an Oocyte-Produced Signal Required for Maintenance of the Adult Female Sexual Phenotype in Zebrafish. Mullins MC, editor. PLOS Genet. 2016 Sep 19;12(9):e1006323.

13. Wilson CA, High SK, McCluskey BM, Amores A, Yan YL, Titus TA, et al. Wild sex in zebrafish: Loss of the natural sex determinant in domesticated strains. Vol. 198, Genetics. 2014. 1291–1308 p.

14. Dranow DB, Tucker RP, Draper BW. Germ cells are required to maintain a stable sexual phenotype in adult zebrafish. Dev Biol. 2013 Apr;376(1):43–50.

15. Takahashi H. Juvenile hermaphroditism in the zebrafish, Brachydanio rerio. Bull Fac Fish Hokkaido Univ. 1977;28(2):57–65.

16. Leerberg DM, Sano K, Draper BW. Fibroblast growth factor signaling is required for early somatic gonad development in zebrafish. Mullins MC, editor. PLOS Genet. 2017 Sep 5;13(9):e1006993.

17. Braat AK, Zandbergen T, Van De Water S, Goos HJTH, Zivkovic D. Characterization of zebrafish primordial germ cells: Morphology and early distribution of vasa RNA. Dev Dyn. 1999;216(2):153–67.

18. DeFalco T, Bhattacharya I, Williams AV, Sams DM, Capel B. Yolk-sac-derived macrophages regulate fetal testis vascularization and morphogenesis. Proc Natl Acad Sci. 2014;111(23):E2384–93.

481 19. Brennan J, Karl J, Capel B. Divergent Vascular Mechanisms Downstream of Sry Establish
482 the Arterial System in the XY Gonad. Dev Biol. 2002 Apr;244(2):418–28.

483 20. Garcia-Alonso L, Lorenzi V, Mazzeo CI, Alves-Lopes JP, Roberts K, Sancho-Serra C, et al.
484 Single-cell roadmap of human gonadal development. Nature. 2022 Jul 1;607(7919):540–7.

485 21. Liu Y, Kossack ME, McFaul ME, Christensen LN, Siebert S, Wyatt SR, et al. Single-cell
486 transcriptome reveals insights into the development and function of the zebrafish ovary.
487 eLife. 2022 May 19;11:e76014.

488 22. Westerfield M. The zebrafish book: A guide for the laboratory use of zebrafish Danio
489 (Brachydanio) rerio. Eugene, OK: Westerfield, M; 2007.

490 23. Kossack ME, Manz KE, Martin NR, Pennell KD, Plavicki J. Environmentally relevant uptake,
491 elimination, and metabolic changes following early embryonic exposure to 2,3,7,8-
492 tetrachlorodibenzo-p-dioxin in zebrafish. Chemosphere. 2022;136723.

493 24. Kimmel CB, Ballard WW, Kimmel SR, Ullmann B, Schilling TF. Stages of embryonic
494 development of the zebrafish. Dev Dyn. 1995 Jul;203(3):253–310.

495 25. Singleman C, Holtzman NG. Growth and maturation in the zebrafish, Danio rerio: a staging
496 tool for teaching and research. Zebrafish. 2014/06/30 ed. 2014 Aug;11(4):396–406.

497 26. Roman BL, Pham VN, Lawson ND, Kulik M, Childs S, Lekven AC, et al. Disruption of acvrl1
498 increases endothelial cell number in zebrafish cranial vessels. Development.
499 2002;129(12):3009–19.

500 27. Choi J, Dong L, Ahn J, Dao D, Hammerschmidt M, Chen JN. FoxH1 negatively modulates
501 flk1 gene expression and vascular formation in zebrafish. Dev Biol. 2007 Apr
502 15;304(2):735–44.

503 28. Kikuchi K, Holdway JE, Major RJ, Blum N, Dahn RD, Begemann G, et al. Retinoic Acid
504 Production by Endocardium and Epicardium Is an Injury Response Essential for Zebrafish
505 Heart Regeneration. Dev Cell. 2011 Mar;20(3):397–404.

506 29. Jung HM, Castranova D, Swift MR, Pham VN, Venero Galanternik M, Isogai S, et al.
507 Development of the larval lymphatic system in zebrafish. Dev Camb. 2017;144(11):2070–
508 81.

509 30. Okuda KS, Astin JW, Misa JP, Flores MV, Crosier KE, Crosier PS. Lyve1 expression
510 reveals novel lymphatic vessels and new mechanisms for lymphatic vessel development in
511 zebrafish. Dev Camb. 2012;139(13):2381–91.

512 31. Leu DH, Draper BW. The ziwi promoter drives germline-specific gene expression in
513 zebrafish. Dev Dyn. 2010 Aug 24;239(10):2714–21.

514 32. Ando K, Fukuhara S, Izumi N, Nakajima H, Fukui H, Kelsh RN, et al. Clarification of mural
515 cell coverage of vascular endothelial cells by live imaging of zebrafish. Development. 2016
516 Jan 1;dev.132654.

517 33. Ellett F, Pase L, Hayman JW, Andrianopoulos A, Lieschke GJ. mpeg1 promoter transgenes
518 direct macrophage-lineage expression in zebrafish. Blood. 2011 Jan 27;117(4):e49–56.

519 34. Davison JM, Akitake CM, Goll MG, Rhee JM, Gosse N, Baier H, et al. Transactivation from
520 Gal4-VP16 transgenic insertions for tissue-specific cell labeling and ablation in zebrafish.
521 Dev Biol. 2007;304(2):811–24.

522 35. Hao Y, Hao S, Andersen-Nissen E, Mauck WM, Zheng S, Butler A, et al. Integrated analysis
523 of multimodal single-cell data. Cell. 2021 Jun;184(13):3573-3587.e29.

524 36. Satija R, Farrell JA, Gennert D, Schier AF, Regev A. Spatial reconstruction of single-cell
525 gene expression data. Nat Biotechnol. 2015;33(5):495–502.

526 37. Shih YH, Portman D, Idrizi F, Grosse A, Lawson ND. Integrated molecular analysis identifies
527 a conserved pericyte gene signature in zebrafish. Development. 2021 Dec
528 7;148(23):dev200189.

529 38. Padberg Y, Schulte-Merker S, van Impel A. The lymphatic vasculature revisited—new
530 developments in the zebrafish. Methods Cell Biol. 2017;138:221–38.

531 39. Astin JW, Haggerty MJ, Okuda KS, Le Guen L, Misa JP, Tromp A, et al. Vegfd can
532 compensate for loss of Vegfc in zebrafish facial lymphatic sprouting. Development.
533 2014;141(13):2680–90.

534 40. Bussmann J, Bos FL, Urasaki A, Kawakami K, Duckers HJ, Schulte-Merker S. Arteries
535 provide essential guidance cues for lymphatic endothelial cells in the zebrafish trunk.
536 Development. 2010 Aug 15;137(16):2653–7.

537 41. Cha YR, Fujita M, Butler M, Isogai S, Kochhan E, Siekmann AF, et al. Chemokine signaling
538 directs trunk lymphatic network formation along the preexisting blood vasculature. Dev Cell.
539 2012;22(4):824–36.

540 42. Hogan BM, Bos FL, Bussmann J, Witte M, Chi NC, Duckers HJ, et al. Ccbe1 is required for
541 embryonic lymphangiogenesis and venous sprouting. Nat Genet. 2009;41(4):396–8.

542 43. Nicenboim J, Malkinson G, Lupo T, Asaf L, Sela Y, Mayseless O, et al. Lymphatic vessels
543 arise from specialized angioblasts within a venous niche. Nature. 2015;522(7554):56–61.

544 44. van Impel A, Zhao Z, Hermkens DM, Roukens MG, Fischer JC, Peterson-Maduro J, et al.
545 Divergence of zebrafish and mouse lymphatic cell fate specification pathways.
546 Development. 2014;141(6):1228–38.

547 45. Yaniv K, Isogai S, Castranova D, Dye L, Hitomi J, Weinstein BM. Imaging the developing
548 lymphatic system using the zebrafish. In Chichester; New York; John Wiley; 1999; 2007. p.
549 139.

550 46. Küchler AM, Gjini E, Peterson-Maduro J, Cancilla B, Wolburg H, Schulte-Merker S.
551 Development of the zebrafish lymphatic system requires VEGFC signaling. Curr Biol.
552 2006;16(12):1244–8.

553 47. Kaipainen A, Korhonen J, Mustonen T, van Hinsbergh VW, Fang GH, Dumont D, et al.
554 Expression of the fms-like tyrosine kinase 4 gene becomes restricted to lymphatic
555 endothelium during development. Proc Natl Acad Sci. 1995 Apr 11;92(8):3566–70.

556 48. Karkkainen MJ, Haiko P, Sainio K, Partanen J, Taipale J, Petrova TV, et al. Vascular
557 endothelial growth factor C is required for sprouting of the first lymphatic vessels from
558 embryonic veins. Nat Immunol. 2004 Jan;5(1):74–80.

559 49. Koltowska K, Lagendijk AK, Pichol-Thievend C, Fischer JC, Francois M, Ober EA, et al.
560 Vegfc Regulates Bipotential Precursor Division and Prox1 Expression to Promote Lymphatic
561 Identity in Zebrafish. Cell Rep. 2015;13(9):1828–41.

562 50. Villefranc JA, Nicoli S, Bentley K, Jeltsch M, Zarkada G, Moore JC, et al. A truncation allele
563 in vascular endothelial growth factor c reveals distinct modes of signaling during lymphatic
564 and vascular development. Development. 2013 Apr 1;140(7):1497–506.

565 51. Ferrara N, Gerber HP, LeCouter J. The biology of VEGF and its receptors. Nat Med. 2003
566 Jun 1;9(6):669–76.

567 52. Das RN, Tevet Y, Safriel S, Han Y, Moshe N, Lambiase G, et al. Generation of specialized
568 blood vessels via lymphatic transdifferentiation. Nature. 2022 Jun 16;606(7914):570–5.

569 53. Fong GH, Rossant J, Gertsenstein M, Breitman ML. Role of the Flt-1 receptor tyrosine
570 kinase in regulating the assembly of vascular endothelium. Nature. 1995 Jul;376(6535):66–
571 70.

572 54. Bahrami N, Childs SJ. Pericyte biology in zebrafish. Adv Exp Med Biol. 2018;1109:33–51.

573 55. Robinson RS, Woad KJ, Hammond AJ, Laird M, Hunter MG, Mann GE. Angiogenesis and
574 vascular function in the ovary. Reproduction. 2009 Dec;138(6):869–81.

575 56. Seynhaeve ALB, Oostinga D, van Haperen R, Eilken HM, Adams S, Adams RH, et al.
576 Spatiotemporal endothelial cell – pericyte association in tumors as shown by high resolution
577 4D intravital imaging. Sci Rep. 2018 Dec;8(1):9596.

578 57. Svingen T, Koopman P. Building the mammalian testis: origins, differentiation, and
579 assembly of the component cell populations. Genes Dev. 2013 Nov 15;27(22):2409–26.

580 58. Jokela H, Lokka E, Kiviranta M, Tyystjärvi S, Gerke H, Elima K, et al. Fetal-derived
581 macrophages persist and sequentially maturate in ovaries after birth in mice. Eur J Immunol.
582 2020 Oct;50(10):1500–14.

583 59. Zhang Z, Huang L, Brayboy L. Macrophages: an indispensable piece of ovarian health. Biol
584 Reprod. 2021 Mar 11;104(3):527–38.

585 60. Coveney D, Cool J, Oliver T, Capel B. Four-dimensional analysis of vascularization during
586 primary development of an organ, the gonad. Proc Natl Acad Sci. 2008;105(20):7212–7.

587 61. Brown HM, Robker RL, Russell DL. Development and Hormonal Regulation of the Ovarian
588 Lymphatic Vasculature. Endocrinology. 2010 Nov 1;151(11):5446–55.

589 62. Svingen T, François M, Wilhelm D, Koopman P. Three-Dimensional Imaging of Prox1-EGFP
590 Transgenic Mouse Gonads Reveals Divergent Modes of Lymphangiogenesis in the Testis
591 and Ovary. Mallo M, editor. PLoS ONE. 2012 Dec 20;7(12):e52620.

592 63. Wiens KM, Lee HL, Shimada H, Metcalf AE, Chao MY, Lien CL. Platelet-Derived Growth
593 Factor Receptor β Is Critical for Zebrafish Intersegmental Vessel Formation. Hendricks M,
594 editor. PLoS ONE. 2010 Jun 25;5(6):e11324.

595 64. Bower NI, Koltowska K, Pichol-Thievend C, Virshup I, Paterson S, Lagendijk AK, et al.
596 Mural lymphatic endothelial cells regulate meningeal angiogenesis in the zebrafish. Nat
597 Neurosci. 2017;20(6):774–83.

598 65. Redmer DA, Reynolds LP. Angiogenesis in the ovary. Rev Reprod. 1996;1(3):182–92.

599 66. Israely T, Dafni H, Granot D, Nevo N, Tsafriri A, Neeman M. Vascular remodeling and
600 angiogenesis in ectopic ovarian transplants: A crucial role of pericytes and vascular smooth
601 muscle cells in maintenance of ovarian grafts. Biol Reprod. 2003;68(6):2055–64.

602 67. Chiaverina G, di Blasio L, Monica V, Accardo M, Palmiero M, Peracino B, et al. Dynamic
603 Interplay between Pericytes and Endothelial Cells during Sprouting Angiogenesis. Cells.
604 2019;8(9):1–13.

605 68. Kofler N, Naiche LA, Zimmerman LD, Kitajewski JK. Inhibition of Jagged-Specific Notch
606 Activation Reduces Luteal Angiogenesis and Causes Luteal Hemorrhaging of Hormonally
607 Stimulated Ovaries. ACS Pharmacol Transl Sci. 2019;2(5):325–32.

608 69. Hall AP, Ashton S, Horner J, Wilson Z, Reens J, Richmond GHP, et al. PDGFR Inhibition
609 Results in Pericyte Depletion and Hemorrhage into the Corpus Luteum of the Rat Ovary.
610 Toxicol Pathol. 2016;44(1):98–111.

611 70. Hess KA, Chen L, Larsen WJ. The ovarian blood follicle barrier is both charge- and size-
612 selective in mice. Biol Reprod. 1998;58(3):705–11.

613 71. Siu MKY, Cheng CY. The Blood-Follicle Barrier (BFB) in disease and in ovarian function.
614 Adv Exp Med Biol. 2013;763:186–92.

615 72. Gaengel K, Niaudet C, Hagikura K, Laviña B, Muhl L, Hofmann JJ, et al. The Sphingosine-
616 1-Phosphate Receptor S1PR1 Restricts Sprouting Angiogenesis by Regulating the Interplay
617 between VE-Cadherin and VEGFR2. Dev Cell. 2012 Sep;23(3):587–99.

618 73. Yanagida K, Liu CH, Faraco G, Galvani S, Smith HK, Burg N, et al. Size-selective opening
619 of the blood–brain barrier by targeting endothelial sphingosine 1–phosphate receptor 1.
620 Proc Natl Acad Sci. 2017 Apr 25;114(17):4531–6.

621 74. Wang X, Qiu Z, Dong W, Yang Z, Wang J, Xu H, et al. S1PR1 induces metabolic
622 reprogramming of ceramide in vascular endothelial cells, affecting hepatocellular carcinoma
623 angiogenesis and progression. Cell Death Dis. 2022 Sep 6;13(9):768.

624 75. Pascuali N, Scotti L, Oubiña G, de Zúñiga I, Gomez Peña M, Pomilio C, et al. Platelet-
625 derived growth factor B restores vascular barrier integrity and diminishes permeability in
626 ovarian hyperstimulation syndrome. Mol Hum Reprod. 2020 Aug 1;26(8):585–600.

76. Di Pietro M, Pascuali N, Parborell F, Abramovich D. Ovarian angiogenesis in polycystic ovary syndrome. Reproduction. 2018;155(5):R199–209.

77. Zaidi J, Campbell S, Pittrof R, Kyei-Mensah A, Shaker A, S.Jacobs H, et al. Contraception: Ovarian stromal blood flow in women with polycystic ovaries—a possible new marker for diagnosis? Hum Reprod. 1995 Aug 1;10(8):1992–6.

78. Yan YL, Desvignes T, Bremiller R, Wilson C, Dillon D, High S, et al. Gonadal soma controls ovarian follicle proliferation through Gsdf in zebrafish. Dev Dyn. 2017 Nov;246(11):925–45.

79. Fantin A, Vieira JM, Gestri G, Denti L, Schwarz Q, Prykhozhij S, et al. Tissue macrophages act as cellular chaperones for vascular anastomosis downstream of VEGF-mediated endothelial tip cell induction. Blood. 2010 Aug 5;116(5):829–40.

80. Eubank TD, Galloway M, Montague CM, Waldman WJ, Marsh CB. M-CSF Induces Vascular Endothelial Growth Factor Production and Angiogenic Activity From Human Monocytes 1. J Immunol. 2003 Sep 1;171(5):2637–43.

81. Rymo SF, Gerhardt H, Wolfhagen Sand F, Lang R, Uv A, Betsholtz C. A Two-Way Communication between Microglial Cells and Angiogenic Sprouts Regulates Angiogenesis in Aortic Ring Cultures. PLOS ONE. 2011 Jan 10;6(1):e15846.

82. Martin P, Gurevich DB. Macrophage regulation of angiogenesis in health and disease. Spec Issue Muscle Growth Regen Kathryn Wagner Spec Issue Role Macrophages Tissue Homeost Benedicte Chazaud. 2021 Nov 1;119:101–10.

83. Sunderkötter C, Goebeler M, Schulze-Osthoff K, Bhardwaj R, Sorg C. Macrophage-derived angiogenesis factors. Pharmacol Ther. 1991 Jan 1;51(2):195–216.

84. Wu R. Macrophage contributions to ovarian function. Hum Reprod Update. 2004 Mar 1;10(2):119–33.

85. Ono Y, Nagai M, Yoshino O, Koga K, Nawaz A, Hatta H, et al. CD11c+ M1-like macrophages (MΦs) but not CD206+ M2-like MΦ are involved in folliculogenesis in mice ovary. Sci Rep. 2018 Dec;8(1):8171.

Figure legends:

Figure 1. Vascular Endothelial Cells in the Bipotential Gonad. (A-H) Representative images showing the defined 3 categories for describing the relationship between vascular endothelial cells and germ cells in the biopotential gonad: “No Contact” (**A**), “proximal” (**B-C**; open arrowhead), and “Contact” (**D-E**; red arrow). All images are oriented with anterior (A) to the left and posterior (P) to the right. (**F**) The relationship between the vascular endothelial cells and the

661 germ cells was categorized in individuals from multiple independent spawning events and
662 correlated with age (see Supplemental Table S1). Vascularization of the gonad occurs in most
663 individuals by 20 dpf. (**G**) Standard length is a more accurate measure of development. Most
664 fish had vascularized gonads when they reached a standard length of 7.21±0.666mm. (**H**) The
665 main vessel supplying the gonad with blood, the gonadal artery (white arrowheads), originates
666 from the swim bladder artery (red arrowheads). (**I**) A schematic representing the GA and SBA in
667 the context of the body cavity. VEC = Vascular Endothelial Cell, AC = Anterior Chamber, SBA =
668 Swim Bladder Artery, PD = Pneumatic Duct, AC = Anterior Chamber, PC = Posterior Chamber.
669 Scale = 100 μm.
670
671 **Figure 2. The primary stromal cell populations are present in the gonad when fish reach a**
672 **standard length of approximately 7mm**. (**A**) At each age, individuals from multiple spawns
673 were collected to determine if there was contact between the stromal cell of interest and the
674 germ cells. Vascular endothelial cells (red circle), Lymphatic endothelial cells (green triangle),
675 Pericytes (blue square), and macrophage (purple diamonds) all reach the gonad at
676 approximately the same time, 15-20 dpf. (**B**) Each fish was measured before dissection for the
677 standard length which corresponds to its development. The full list of replicates, individuals,
678 average length, and observations can be found in **Supplemental Table S1**.
679
680 **Figure 3. Endothelial gene expression in 40 dpf ovary. (A)** Expression of vascular
681 endothelial cell genes *kdrl, fli1*, and *flt1* occurs in a majority of the endothelial cells. (**B**)
682 lymphatic endothelial genes *lyve1b*, *flt4*, and *prox1* are expressed in a smaller subset of cells.
683 (**C**) There is no overlap in expression of *kdrl* (red) and *lyve1b* (green) by single-cell sequencing,
684 expression overlap is shown in yellow as demonstrated in the fourth pane. (**D**) There is overlap
685 in expression of *flt4* (red) and *lyve1b* (green) suggesting that lymphatic endothelial cells
686 originate canonically.

687

688 **Figure 4. *kdrl* and *mrc1a* are co-expressed in the 20 dpf ovary.** (**A**) Maximum intensity
689 projection of the 20 dpf gonad (germ cells = blue, gonad outlined) showing overlap in *kdrl*
690 (magenta) and *mrc1a* (green) expression. (**B**) Single channel showing *kdrl* expression alone
691 suggests that *kdrl* is expressed in all cells. (**C**) Single channel showing *mrc1a* expression is
692 inversely correlate with the strength of *kdrl* expression. (**D**) Orthogonal slice of the maximum
693 intensity projection shows that the expression of both markers is overlapping within cells. (**E**)
694 Co-localization analysis of the cells circled in red in (**F**) showing expression of *kdrl* and *mrc1a* is
695 highly correlated. Scale = 20 μm.

696

697 **Figure 5. The *pdgfrb*+ expression domain encompasses multiple ovarian stromal cell**
698 **types**. In the embryo, cluster 39 (pink) represents a subset of *pdgfrb*+ cells (blue) that are more
699 specific to pericytes. In the ovary, *pdgfrb* is expressed in all ovarian stromal cells (purple), but a
700 subset have more specific pericyte gene expression (yellow).

701

702 **Figure 6. *pdgfrb* positive cells elongate prior to vascular endothelial cells**. Pericytes,
703 labeled with *pdgfrb:EGFP* (green) extend protrusions (white arrows) from existing vessels into
704 the gonad (blue, outlined in white), likely following the endothelial tip cell (magenta). Scale = 20
705 μm

706

707 **Figure 7. Tissue-resident macrophage engulf cells during gonad differentiation.** (**A**)
708 Macrophage can be found in contact with germ cells as early as 12 dpf. (**B**) At 20 dpf,
709 macrophage are abundant in the gonad. (**C**) Macrophage (magenta) are observed removing
710 oocyte material (green) and DNA (white) from the former bipotential gonad (white arrowheads).
711 (**D**) *mpeg1:GAL4; UAS:Kaede* expressing macrophage were photoconverted from green to red

712 (pseudocolored magenta) at 12 dpf. 24 hours after conversion both green and red macrophage
713 could be found in the gonad (blue arrow, outlined). (**E**) Some macrophage in the gonad were
714 only magenta (red arrowhead), indicating that they are resident to the gonad during this period.
715 (**F**) In the green channel, we can observe that some macrophage migrate to the gonad within
716 the 24 hour window post-photoconversion (green arrows). Scale listed.
717

718 **Figures**:

719 **Figure 1.**

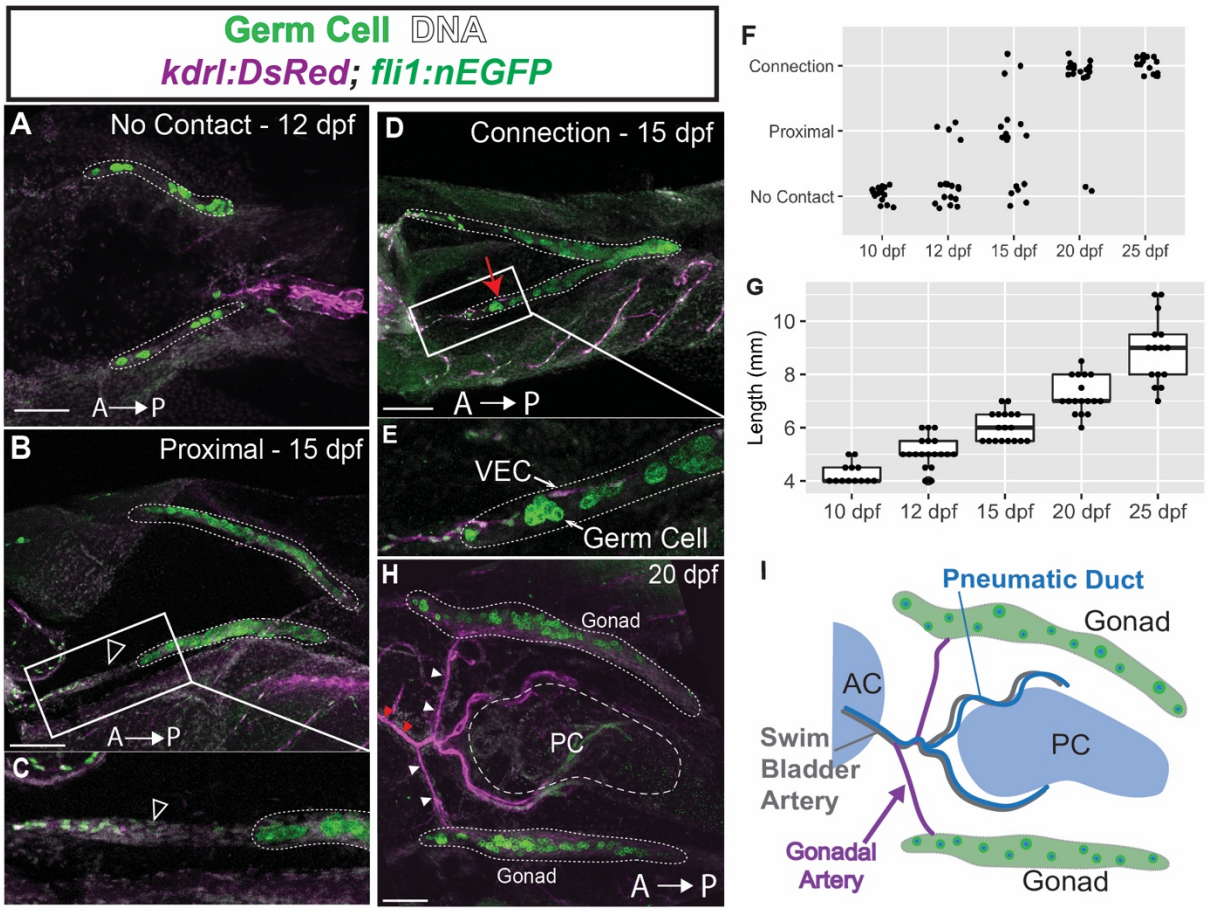

720

721

722 **Figure 2**.

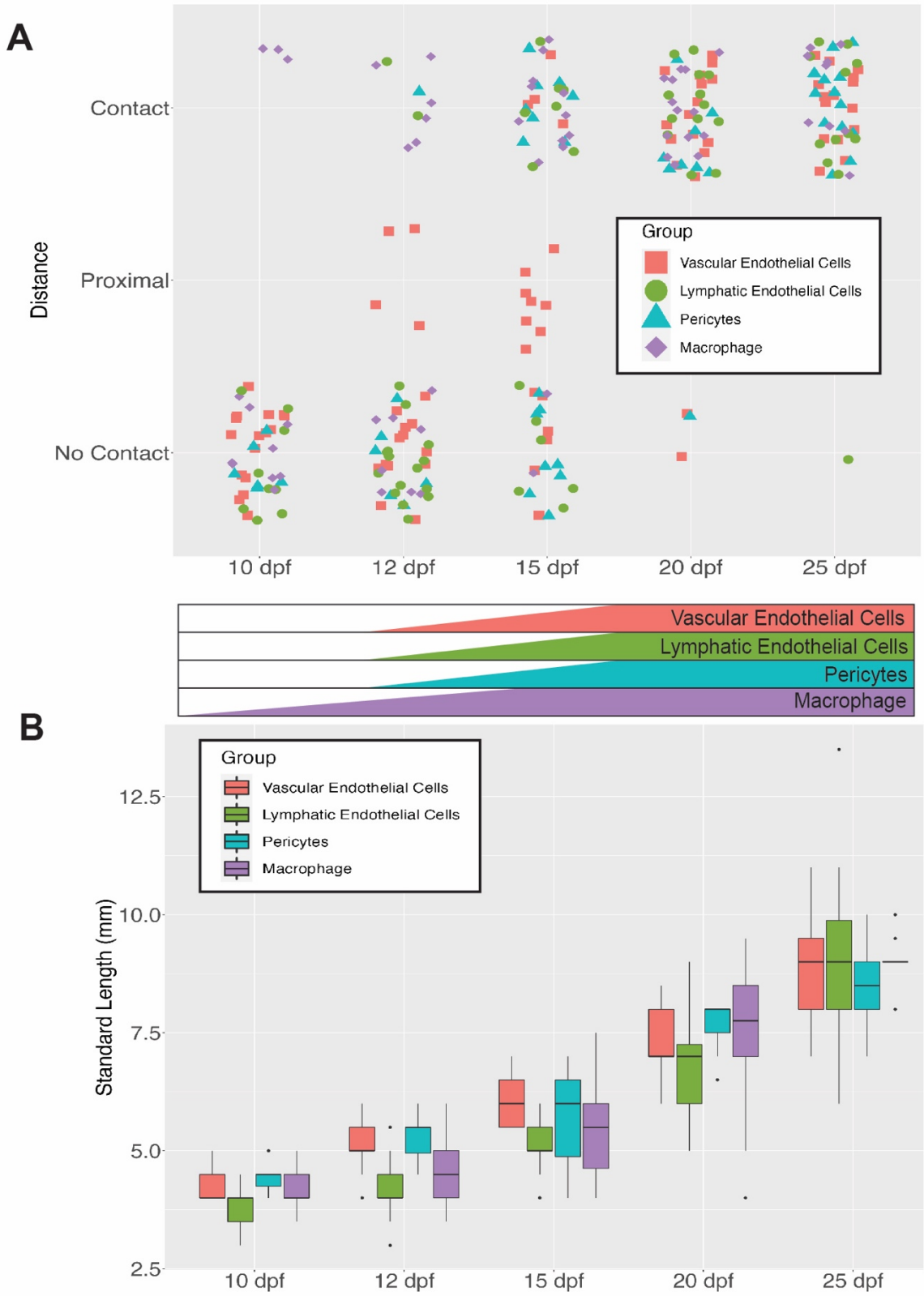

723

Figure 3.

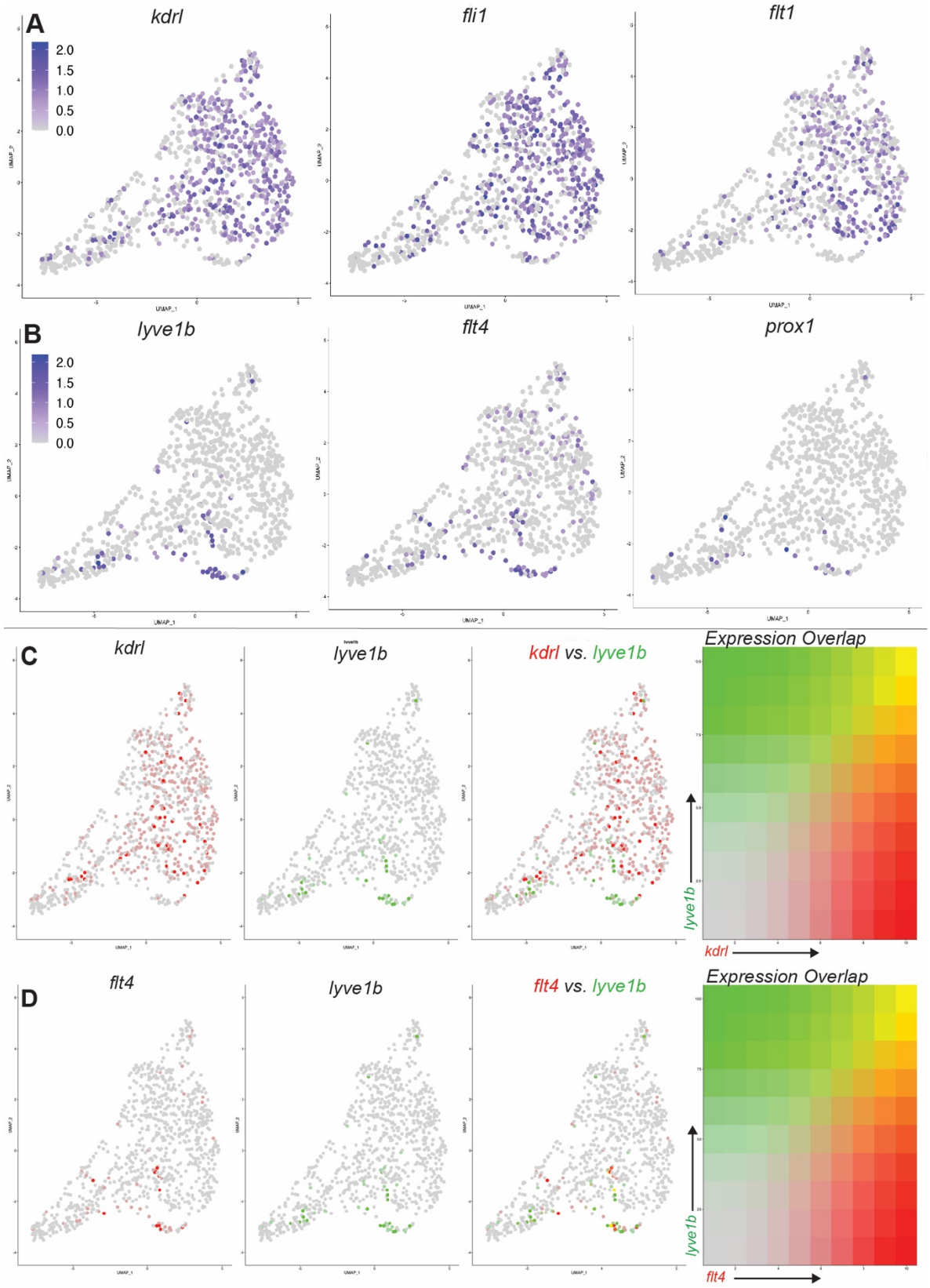
A
kdrl
fli1
flt1
2.0
1.5
1.0
0.5
0.0
B
lyve1b
flt4
prox1
C
kdrl
lyve1b
kdrl vs. lyve1b
Expression Overlap
lyve1b
kdrl
D
flt4
lyve1b
flt4 vs. lyve1b
Expression Overlap
lyve1b
flt4

726 **Figure 4.**

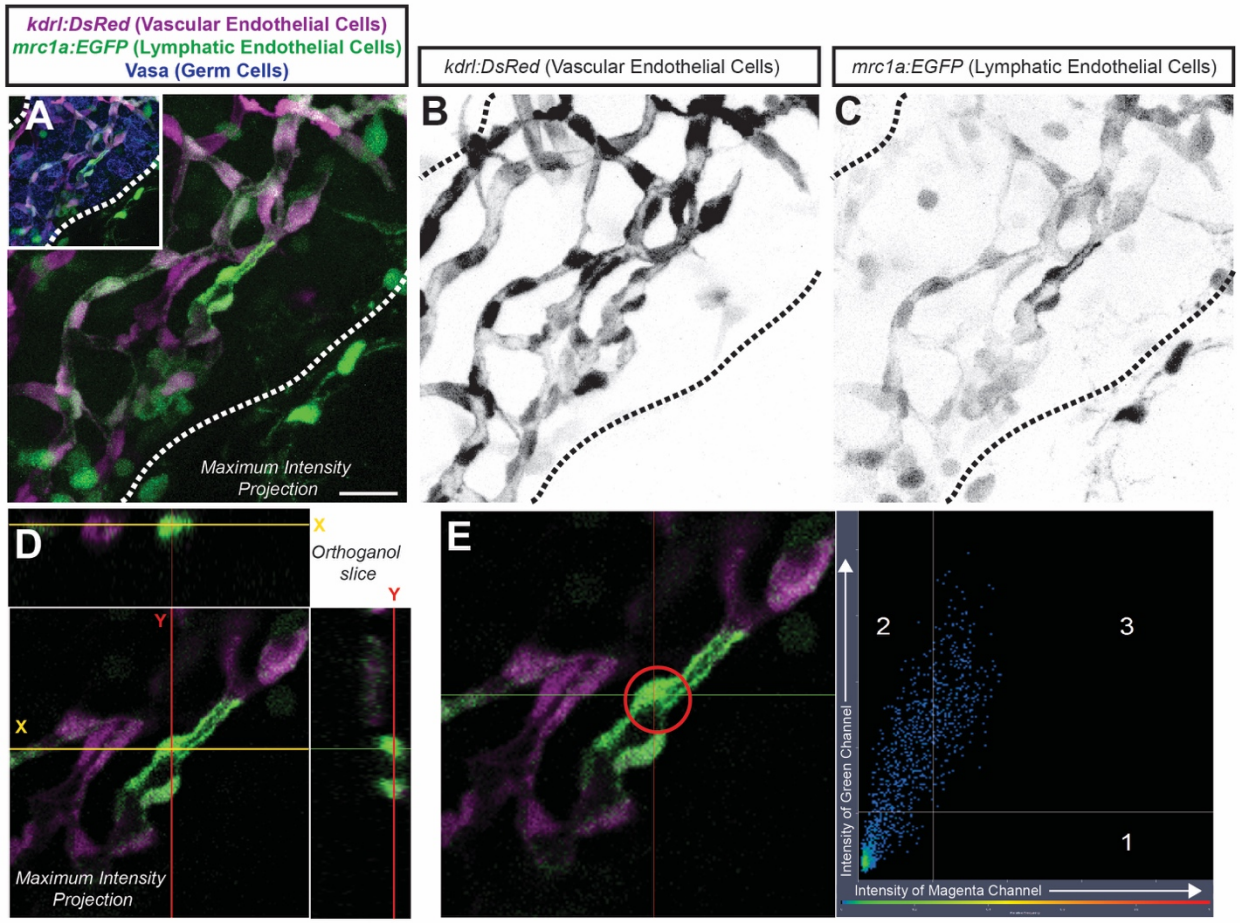

727

728

729 **Figure 5.**

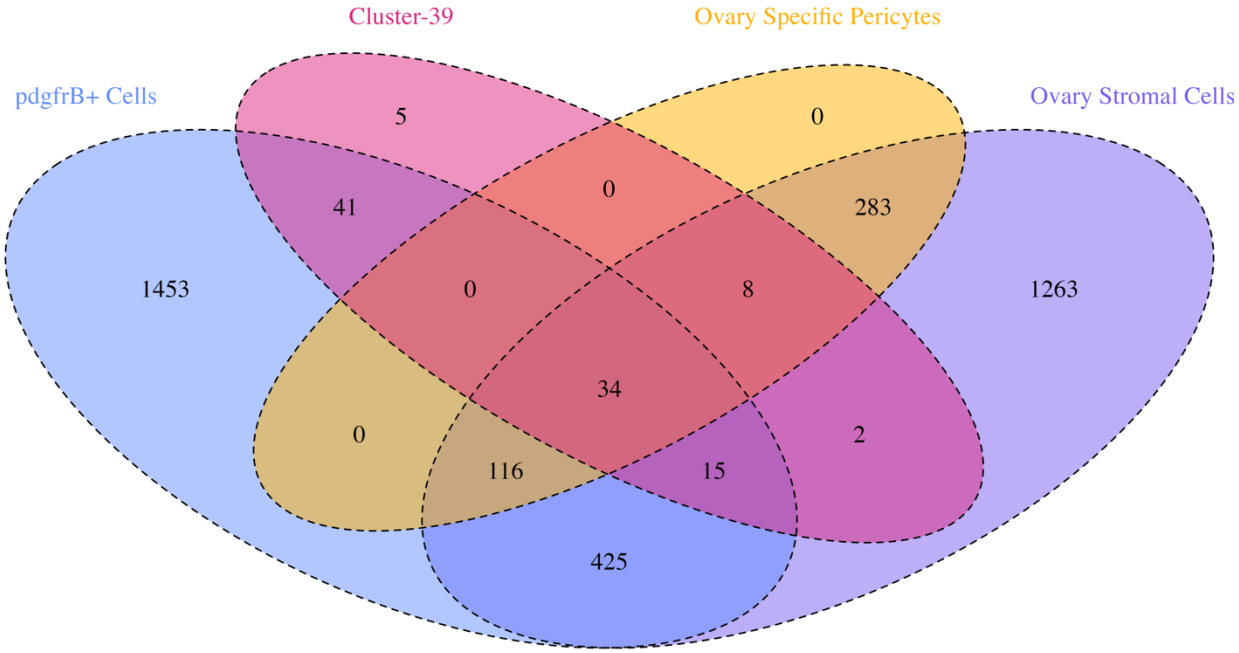

730

731

732

733 **Figure 6**.

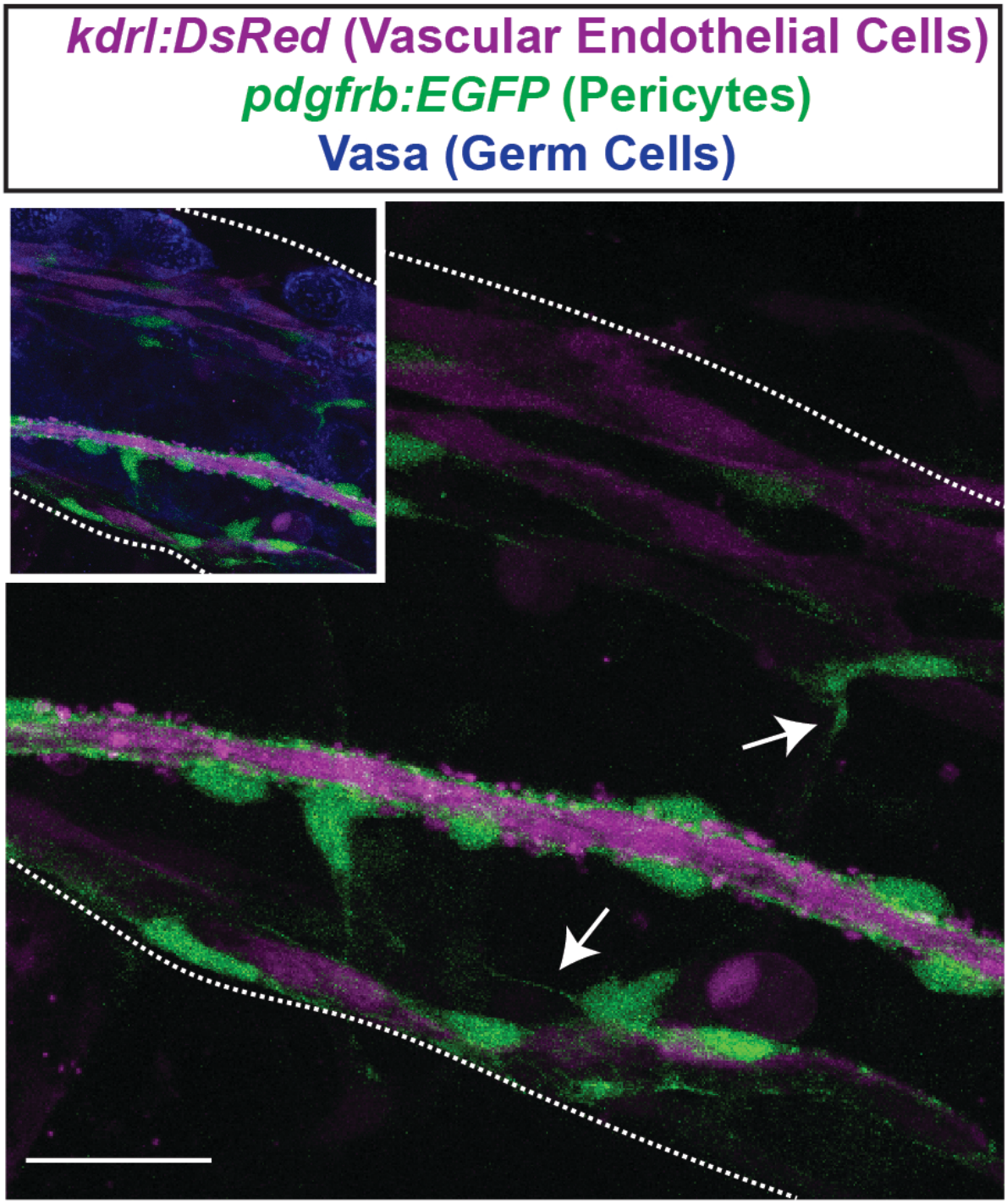

734

735

736 **Figure 7.**

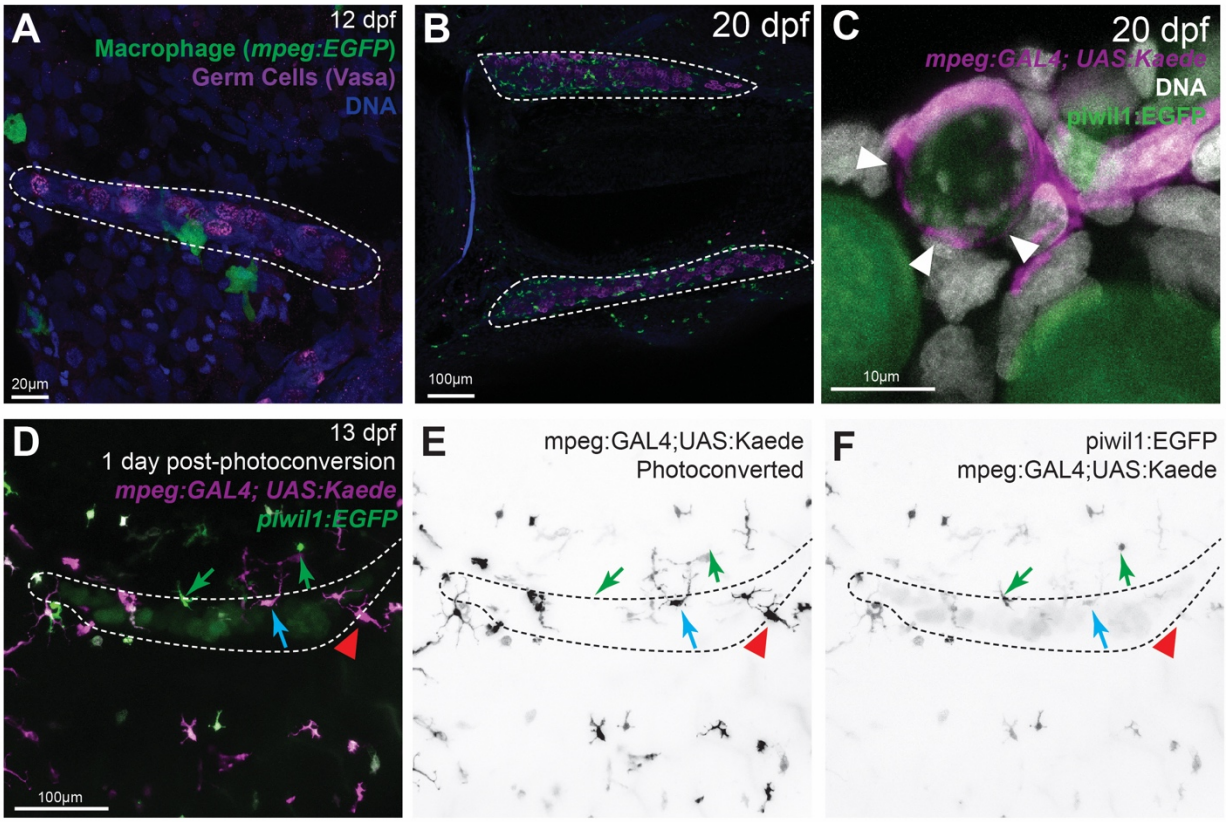

737